Geomechanics and Engineering, *Vol. 21, No. 6 (2020) 503-511*
DOI: https://doi.org/10.12989/gae.2020.21.6.503

Evaluation of side resistance for drilled shafts in rock sections

Cheng-Chieh Hsiao[a], Anjerick J. Topacio[b] and Yit-Jin Chen*

Department of Civil Engineering, Chung Yuan Christian University, Chung-Li District, Taoyuan City 32023, Taiwan

(Received November 26, 2019, Revised April 9, 2020, Accepted April 24, 2020)

Abstract. This study evaluated the side resistance of drilled shafts socketed into rock sections. Commonly used analysis methods for side resistance of piles in rocks are examined by utilizing a large number of load test data. The analysis of the unit side resistance of pile foundations embedded into rock sections is based on an empirical coefficient (α) and the uniaxial compressive strength (q_u) or its root ($\sqrt{q_u}$). The Davisson criterion was used to interpret the resistance capacity from the load test results to acquire the computed relationships. The α–$\sqrt{q_u}$ relationship is proven to be reliable in the prediction of friction resistance. This study further analyzed the relationship by including the effect of rock quality designation (RQD) on the results. Analysis results showed that the analysis model of α–$\sqrt{q_u}$-RQD provided better prediction and reliability considering the RQD classification. Based on these analyses, the side resistance of drilled shafts socked into rocks is provided with statistical data to support the analysis.

Keywords: drilled shaft; load test; friction resistance; rock; rock quality designation

1. Introduction

Limited land for public and housing construction is a current problem worldwide. Creating a high-rise environment, especially in the metros where majority of the population thrive, could be a solution to this problem. With the current construction of increasing high and heavy superstructures, stabilization of the foundation through the construction and installation of deep foundations is a requirement to retain the safety of the system. Several commonly used pile foundations are pre-bored precast piles, driven piles, and drilled shafts. Among these pile types, drilled shaft is often used because it has low noise and vibration during construction and can provide larger diameter and depth for the design than that of other piles. In addition, drilled shafts can easily penetrate rock sections to obtain better bearing capacity.

Piles are usually subjected to loadings, especially from the superstructure. Nevertheless, pile will transmit the load along its length to the soil/rock layer when subjected to axial compression loadings. The side friction and the pile tip resistances generated by the soil/rock layer ultimately support the axial compression load. The side resistance generated by the soil/rock layer originate from the unit side resistance (f_s). The evaluation of f_s of a drilled shaft in the rock section is based on an empirical coefficient (α), which is the adhesion factor, and the uniaxial compressive strength (q_u) or its root ($\sqrt{q_u}$). The α method in rock is similar to the

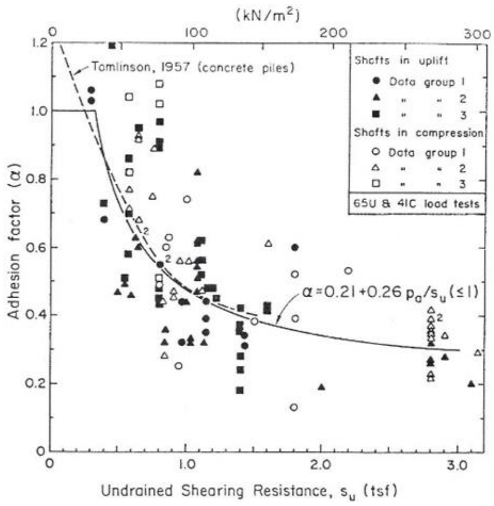

Fig. 1 Early α–s_u relationship (Stas and Kulhawy 1984)

conventional total stress analysis for the side resistance of drilled shaft foundations in cohesive soils, which is related to the average soil undrained shear strength (s_u) over the pile length. Fig. 1 shows the initial α-s_u relationship of the drilled shafts developed by Stas and Kulhawy (1984). However, the s_u values in their analysis were taken from random test types, thus resulting in a scattered relationship. Chen and Kulhawy (1994, 2003) later adopted a unique test type of s_u from consolidated-isotropically undrained triaxial compression (*CIUC*) test [denoted $s_u(CIUC)$] as the reference plane for a consistent test. This approach improved the α_{CIUC}–$s_u(CIUC)$ relationship as demonstrated in Fig. 2. Furthermore, Chen *et al.* (2011) considered the factor of undrained strength ratio ($s_u/\bar{\sigma}_{vm}$) into the correlation of Fig. 2 using the updated load test data (Chen *et al.* 2014), in which $\bar{\sigma}_{vm}$ is the mean effective

*Corresponding author, Ph.D., Professor
E-mail: yjc@cycu.edu.tw
[a]Master Student
[b]Ph.D. Student

ISSN: 2005-307X (Print), 2092-6219 (Online)

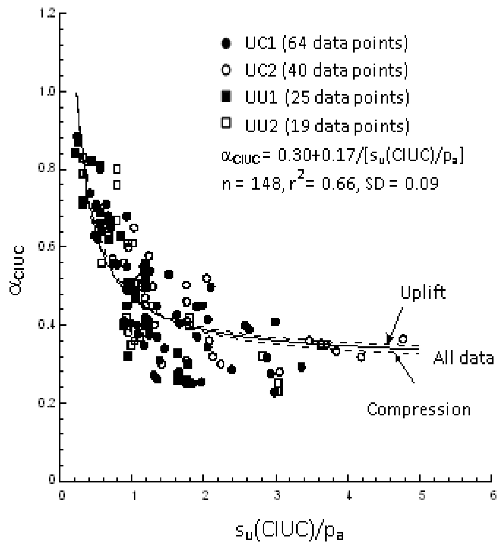

Fig. 2 Improved α_{CIUC}–$s_u(CIUC)$ relationship (Chen and Kulhawy 1994, 2003)

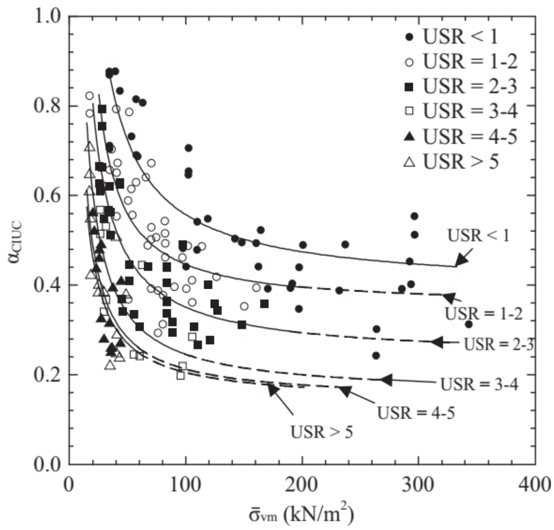

Fig. 3 α_{CIUC}-$s_u(CIUC)/\sigma_{vm}$-σ_{vm} correlations (Chen *et al.* 2011)

overburden stress of pile length. Fig. 3 shows the results of undrained strength ratio (*USR*) correlation, α_{CIUC}-$s_u(CIUC)/\bar{\sigma}_{vm}$-$\bar{\sigma}_{vm}$. Fig. 3 can be regarded as an alternative analysis for traditional α-s_u correlations, especially with a small s_u.

Researchers (e.g., Qian *et al.* 2016, Zhang *et al.* 2017, Rodgers *et al.* 2018, Asem and Gardoni 2019a, b, Chen *et al.* 2019, Marcos and Chen 2019) have studied the interface behavior between pile and ground under axial loading. The analysis methods of unit side resistance are similar between cohesive soils and rocks. For the unit side resistance in rocks, the uniaxial compressive strength of rock (q_u) and its root ($\sqrt{q_u}$) are used instead of s_u. Various investigations were performed and resulted in a variety of relationships in determining the value of f_s of drilled shafts, as listed in Table 1. Kaderabek and Reynolds (1981) suggested that f_s is equal to 0.2 q_u. According to the results of Kulhawy and Goodman (2005), the value of α is recommended to be 0.15

Table 1 Representative analysis models for side resistance in rocks

Empirical Result	Condition	Author
$f_s = 0.30\ (q_u)$	N/A	Kaderabek and Reynolds (1981)
$f_s = 0.15\ (q_u)$	$q_u < 5$ MPa	Kulhawy and Goodman (1987)
$f_s = (0.2\sim0.3)\ (\sqrt{q_u})$	$q_u < 40$ MPa	Horvath *et al.* (1983)
$f_s = 1.886\ (q_u/p_a)^{0.5}$	for rough surface	Rowe and Armitage (1987)
$f_s = (0.03\sim0.04)\ (\sqrt{q_u})$	$q_u < 40$ MPa	AASHTO (1992)
$f_s = 0.15\ (\sqrt{q_u})$	0.25 MPa < q_u < 3 MPa	Hooley and Lefroy-Brooks (1993)
$f_s = (0.16\sim0.21)\ (\sqrt{q_u})$	N/A	Ku *et al.* (2004)
$f_s = (0.1\sim0.5)\ (\sqrt{q_u})$	N/A	Yang *et al.* (2010)

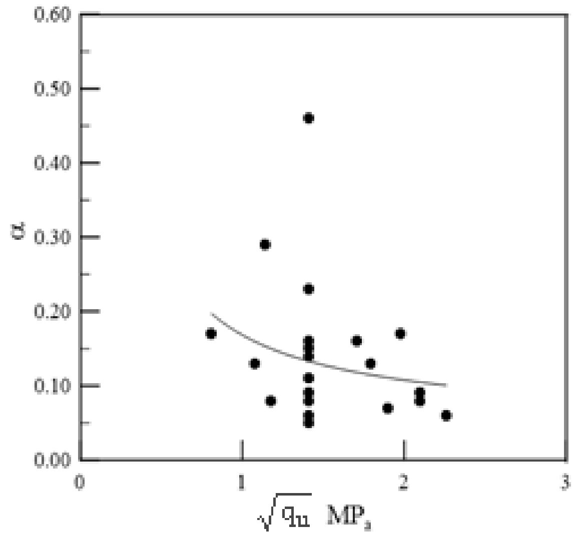

Fig. 4 α–$\sqrt{q_u}$ relationship (Yang *et al.* 2010)

and that of q_u should be less than 5 MPa. Their research utilized the uniaxial compressive strength in determining the side resistance.

Other researchers utilized the $\sqrt{q_u}$ in determining unit side resistances. Horvath *et al.* (1983) also suggested that the value of q_u should be less than 40 MPa and that of α should range from 0.2 to 0.3. Rowe and Armitage (1987) established the equation as normalized by atmospheric stress (1 p_a = 101.3 kN/m^2). AASHTO (1992) suggested that the value of q_u should be less than 40 MPa and that of α should range from 0.03 to 0.04. Hooley and Lefroy-Brooks (1993) studied friction of piles in over-compacted clay, soft rock, and weathered rock and recommended that the value of q_u is between 0.25 and 3.0 MPa and that of α value is 0.15. Ku *et al.* (2004) conducted a related research on western soft rocks of Taiwan and recommended that α value should range from 0.16 to 0.21. However, they did not recommend any range for the value of q_u. Last, Yang *et al.* (2010) found that the α value of piles socketed into rocks in northern Taiwan ranges from 0.1 to 0.5, with no range for the value of q_u.

Fig. 4 shows that the current range of the α coefficient values is broad and the reliability of the relationship is

Table 2 Basic information of axial compression load tests data for analysis

Shaft No.	Test site	Rock description	*RQD* (%)	Depth, D (m)	Diameter, B (m)	Test depth (GL-m)	q_u[a] (MPa)	$\sqrt{q_u}$	f_s[b] (MPa)	α[c]	α[d]
TP1	Zhonghe, New Taipei, Taiwan	Tuff	50~75	37.6	1.95[e]	28.0 ~ 36.0	12.77	3.57	0.59	0.05	0.17
TP2	Zhonghe, New Taipei, Taiwan	Tuff	50~75	42.6	1.95[e]	34.2 ~ 41.0	10.01	3.16	0.51	0.05	0.16
TP3	Taichung, Taiwan	Soft sandstone	50~75	20.0	1.20	4.0 ~ 19.0	0.60	0.77	0.14	0.23	0.18
TP4	Xinyi, Taipei, Taiwan	Sandstone	50~75	66.0	1.50	61.5 ~ 66.0	4.17	2.04	0.33	0.08	0.16
TP5	Zhonghe, New Taipei, Taiwan	Sandstone	90~100	25.5	1.50	21.5 ~ 25.5	0.20	0.45	0.16	0.80	0.36
TP6	Nangang, Taipei, Taiwan	Soft sandstone	90~100	48.0	1.50	40.0 ~ 48.0	1.21	1.10	0.29	0.24	0.26
TP7	Nangang, Taipei, Taiwan	Soft sandstone	90~100	48.0	1.50	40.0 ~ 48.0	0.80	0.89	0.24	0.30	0.27
TP8	Neihu, Taipei, Taiwan	Sandstone	90~100	53.0	1.50	49.5 ~ 53.0	1.03	1.01	0.27	0.26	0.27
TP9	Daan, Taipei, Taiwan	Sandstone	25~50	30.0	1.20	26.4 ~ 30.0	2.26	1.50	0.19	0.08	0.13
TP10	Nangang, Taipei, Taiwan	Weathered sandstone	25~50	53.5	2.00	37.2 ~ 53.3	2.46	1.57	0.20	0.08	0.13
TP11	Nangang, Taipei, Taiwan	Weathered sandstone	25~50	54.5	2.00	38.2 ~ 54.5	0.34	0.58	0.09	0.26	0.15
TP12	Xinyi, Taipei, Taiwan	Medium sandstone	25~50	48.0	1.50	47.7 ~ 52.0	0.65	0.81	0.13	0.20	0.16
TP13	Xinyi, Taipei, Taiwan	Soft sandstone	75~90	47.7	1.20	41.7 ~ 47.7	0.16	0.40	0.13	0.81	0.33
TP14	Xinyi, Taipei, Taiwan	Soft sandstone	50~75	59.0	1.20	55.8 ~ 59.0	3.00	1.73	0.27	0.09	0.16
TP15	Xinyi, Taipei, Taiwan	Soft sandstone	50~75	29.0	1.20	24.9 ~ 29.0	0.13	0.36	0.08	0.62	0.22
TP16	Nangang, Taipei, Taiwan	Sandstone	0~25	45.0	1.20	35.0 ~ 42.5	3.47	1.86	0.18	0.05	0.10
TP17	Nangang, Taipei, Taiwan	Sandstone	0~25	38.0	1.99[e]	35.0 ~ 37.4	13.00	3.61	0.37	0.03	0.10
TP18	Zhongshan, Taipei, Taiwan	Sandstone	50~75	60.4	1.50	58.4 ~ 59.8	13.70	3.70	0.54	0.04	0.15
TP19	Zhongshan, Taipei, Taiwan	Sandstone	50~75	48.0	1.50	44.5 ~ 48.0	13.64	3.69	0.64	0.05	0.17
TP20	Zhongshan, Taipei, Taiwan	Sandstone	90~100	46.0	1.29[e]	43.4 ~ 45.3	2.54	1.59	0.31	0.12	0.19
TP21	Anatolia, Turkey	Amphibolite	0~25	10.0	1.20	2.5 ~ 10.0	1.30	1.14	0.14	0.11	0.12
TP22	Anatolia, Turkey	Amphibolite	0~25	9.1	1.20	3.5 ~ 9.1	1.60	1.26	0.15	0.09	0.12
TP23	Anatolia, Turkey	Amphibolite	0~25	8.0	1.20	4.5 ~ 8.0	1.00	1.00	0.13	0.13	TP23
TP24	Xizhi, New Taipei, Taiwan	Sandstone	25~50	25.0	1.00	15.5 ~ 25.5	4.26	2.06	0.33	0.08	TP24
TP25	Zhonghe, New Taipei, Taiwan	Soft sandstone	0~25	17.0	1.80	3.0 ~ 16.4	1.70	1.30	0.17	0.10	0.13
TP26	Zhongzheng, Keelung, Taiwan	Soft sandstone	50~75	36.0	1.00	32.9 ~ 35.4	1.03	1.01	0.17	0.17	0.17
TP27	Wenshan, Taipei, Taiwan	Medium sandstone	0~25	27.5	1.20	25.5 ~ 27.0	1.51	1.23	0.16	0.11	0.13
TP28	Xizhi, New Taipei, Taiwan	Sandstone	90~100	22.8	0.80	12.3 ~ 22.2	0.52	0.72	0.20	0.38	0.28
TP29	Xizhi, New Taipei, Taiwan	Sandstone	0~25	20.4	0.80	15.5 ~ 19.8	1.86	1.36	0.17	0.09	0.12
TP30	Xizhi, New Taipei, Taiwan	Sandstone	75~90	26.4	1.00	16.8 ~ 26.8	0.32	0.57	0.14	0.44	0.25
TP31	Oklahoma, USA	Shale	50~75	8.7	0.70	5.6 ~ 8.8	5.00	2.24	0.37	0.07	0.17
TP32	Oklahoma, USA	Shale	50~75	11.0	0.70	5.6 ~ 11.0	5.00	2.24	0.35	0.07	0.16
TP33	Toscana, Italy	Limestone	25~50	18.5	1.20	11.0 ~ 18.5	0.90	0.95	0.14	0.16	0.15
TP34	Toscana, Italy	Limestone	0~25	39.0	1.20	26 .0 ~ 37.0	3.00	1.73	0.20	0.07	0.12
TP35	Toscana, Italy	Limestone	75~90	13.5	1.20	11.0 ~ 13.5	6.00	2.45	0.44	0.07	0.18
TP36	Singapore	Fragmented siltstone	25~50	7.3	0.70	2.1 ~ 7.3	6.82	2.61	0.25	0.04	0.10
TP37	Singapore	Fragmented siltstone	25~50	13.5	1.40	4 .0~ 10.0	7.00	2.65	0.32	0.05	0.12
TP38	Singapore	Hard shale	25~50	11.5	1.50	3.5 ~ 9.6	7.77	2.79	0.38	0.05	0.14
TP39	Xinyi, Taipei, Taiwan	Soft sandstone	75~90	59.0	1.20	54.6 ~ 58.0	0.26	0.51	0.15	0.58	0.29
TP40	Daan, Taipei, Taiwan	Soft sandstone	75~90	73.0	1.50	67.0 ~ 73.0	0.30	0.55	0.16	0.53	0.29

Table 2 Continued

Shaft No.	Test site	Rock description	RQD (%)	Depth, D (m)	Diameter, B (m)	Test depth (GL-m)	q_u[a] (MPa)	$\sqrt{q_u}$	f_s[b] (MPa)	α[c]	α[d]
TP41	Xinyi, Taipei, Taiwan	Sandstone	90~100	76.0	1.30	71.0 ~ 76.0	0.45	0.67	0.20	0.44	0.30

Note: a: average uniaxial compression strength; b: average unit side resistance; c: adhesion factor for q_u; d: adhesion factor for $\sqrt{q_u}$; e: equivalent diameter

Table 3 Sources of drilled shaft load test data

Shaft No.	References
TP1~2	Midland Development Co. (2015), "Pile load tests for new commercial building of Jingjing section 340, Zhonghe, Xinbei", Taiwan.
TP3	Sinotech Engineering Consultants, Ltd. (2006), "Ultimate pile load test for Contract No. C601, Wuxi No. 4 bridge foundations", Taiwan.
TP4	Great Asia Engineering Consultants, Inc. (2001), "Pile load Test, Unified International Building in Taipei", Taiwan.
TP5	Great Asia Engineering Consultants, Inc. (2004), "Pile load test in the Shanzi section of Zhonghe, Xinbei", Taiwan."
TP6~7	Diagnostic Engineering Consultants, Ltd. (2005), "C10 and C11 new construction project in Nangang software park, Taipei", Taiwan.
TP8	Diagnostic Engineering Consultants, Ltd. (2004), "Songhu EHV power substation, design and construction turnkey project", Taiwan.
TP9	Great Asia Engineering Consultants, Inc. (2006), "Compressive and tensile load tests of pile foundations for dormitory buildings, National Taiwan University", Taiwan.
TP10~11	Cheng, W.C. (2009), "A case history of rock socket pile load testing in Nan-Kang area", Master Thesis, National Taipei University of Technology, Taiwan.
TP12	Sino Geotechnology Inc. (2001), "Pile load test for the F3 base building in Xinyi District, Taipei", Taiwan.
TP13	Sino Geotechnology Inc. (2005), "Pile load test of the 4th landmark (B7 base), Xinyi District, Taipei", Taiwan.
TP14	Diagnostic Engineering Consultants, Ltd. (2005), "Pile load test for the Huaxin Lihua Building in Xinyi District, Taipei", Taiwan.
TP15	Sino Geotechnology Inc. (2003), " Pile load test for the C1 Base building in Xinyi District, Taipei", Taiwan.
TP16-20	Chang, Y.H., Hsieh, J.T., Ro, T.R. & Shih, C.H. (2011), "Construction and load testing of barrette foundations", Sino-Geotechnics, 47-58.
TP21~23	Erol, O., Horoz, A., & Saglamer, A. (2005). "Socket friction capacity of large diameter drilled shafts in highly weathered rock", Proceedings, International Conference on Soil Mechanics and Geotechnical Engineering, 2111-2114.
TP24 & 30	Diagnostic Engineering Consultants, Ltd. (2010), "Pile load test for Yonghe-Xinzhi B-zone new construction project, Xinbei", Taiwan.
TP25	Sino Geotechnology Inc. (2004), "Geological survey and analysis for Shuanghe Hospital at A base, Zhonghe, Xinbei", Taiwan.
TP26	Sanli Engineering Consultants, Ltd. (2014), "Pile load test for National Marine Science and Technology Museum, Keelung", Taiwan.
TP27	Sino Geotechnology Inc. (2003), "Pile load test report for Guotai Royal Garden Project, Wenshan District, Taipei", Taiwan.
TP28~29	Heshe Engineering Co., Ltd. (2014), "Report on the construction of the Beautiful Mountain and Forest Project in Xinzhi, Xinbei", Taiwan.
TP31~32	Goeke, P.M. and Hustad, P.A. (1979), "Instrumented drilled shafts in clay-shale", Proceedings, ASCE Symposium on Deep Foundations, Atlanta,149-165.
TP33~35	Carrubba, P. (1997). "Skin friction of large-diameter piles socketed into rock", Canadian Geotechnical Journal, 34, 230-240.
TP36-38	Radhakrishnan, R. and Leung, C.F. (1989), "Load transfer behavior of rock-socketed piles", Journal of Geotechnical Engineering, ASCE, 115(6), 755-768.
TP39	Great Asia Engineering Consultants, Inc. (2006), "Axial compression and tensile pile load tests of A5 shopping center in Xinyi planning area, Taipei", Taiwan.
TP40	Sino Geotechnology Inc. (2010), "Pile load tests for O3 base in Xinyi Section, Taipei", Taiwan.
TP41	Great Asia Engineering Consultants, Inc. (2005), "Pile load tests for the project of Municipal Government Transfer Station, Taipei", Taiwan.

insufficient. These values may be affected by lithology, rock mass conditions, and the surface condition of the pile body. The current analysis of the frictional value of the pile foundation socketed into rocks is based on the material strength of the rock (q_u). The analysis neglects the other aforementioned factors, possibly affecting the results of the relationship positively.

Thus, a complete assessment of these methods for side resistance analysis of drilled shaft design is reasonable because new approaches have been developed and new parameters can be considered. Additionally, numerous updated load test data have existed since those earlier studies. A broad database was used in the present study to assess the side resistance of drilled shafts embedded into rock layers using the most updated data and approaches. The results were compared statistically and graphically, and then specific design recommendations for the use of unit side resistance in drilled shaft design were presented.

2. Database for analysis

This study collected data from Taiwan and abroad to understand the side resistance behavior of drilled shaft foundations socketed into rock sections. A total of 44 axial compression load test results embedded into rocks,

Table 4 Statistics of drilled shaft load test data

n	Statistics	Pile Geometry		q_u (MPa)	f_s (MPa)
		Pile length D (m)	Pile diameter B (m)		
41	Range	7.30~76.0	0.70-2.00	0.13~13.7	0.08~0.64
	Mean	34.95	1.32	3.51	0.25
	SD	19.24	0.35	3.97	0.14
	COV	0.55	0.26	1.13	0.54

including 27 from sandstones, 3 from mudstones, 3 from limes, 3 from soft sandstones, 3 from hard shales, 2 from tuffs, and 3 from amphibolite, were gathered. The collected pile test information was accompanied by soil (rock) layer information, pile foundation information, load-displacement curves, and load distribution curves along pile length (Hsiao 2018). A shaft is often embedded into the interlayer of soil and rock, but only the side resistance in rock sections is used for analysis in this study. In addition, three load tests in mudstone demonstrated relatively small side resistance. This finding may be attributed to the sensitive characteristics of mudstone to the groundwater, which resulted in larger tip resistance than side resistance. Therefore, the mudstone was not included in the analysis. Only a total of 41 load test results were fit to be utilized as load test data for the analysis.

The basic information of the load test data and their references are summarized in Tables 2 and 3, respectively. Table 4 shows the statistical summary of the database developed from the reports for the interpretation analysis. The shaft construction and test performance were of high quality based on the case history descriptions. Consequently, these data should reflect real field situations, and the analysis results should be representative of application in practice.

3. Method of analysis

Measured load-displacement curves often do not show a clear peak. Thus, a failure criterion should be utilized to define the measured resistance. Davisson offset limit (Davisson 1972) was utilized to obtain the unit side resistance of drilled shafts used in this study because it is widely employed in geotechnical engineering practice. In addition, the method presents consistent results based on the statistics of load test interpretations (Chen and Fang 2009). This method was proposed by comparing the results of wave equation analyses of driven steel piles with static load tests. The load at the intersection of the load-displacement curve with an elastic line offset by 3.8 mm plus the soil quake (pile diameter divided by 120) is identified as the measured resistance. The pile elastic line is PD/AE, in which P = load, D = depth, A = shaft area, E = Young's modulus of shaft. A schematic to interpret the "failure load" (Q_u) is shown in Fig. 5.

The value of α can be back-calculated from the results of interpreted unit side resistance (f_s), as follows:

$$\alpha = f_s / q_u \tag{1}$$

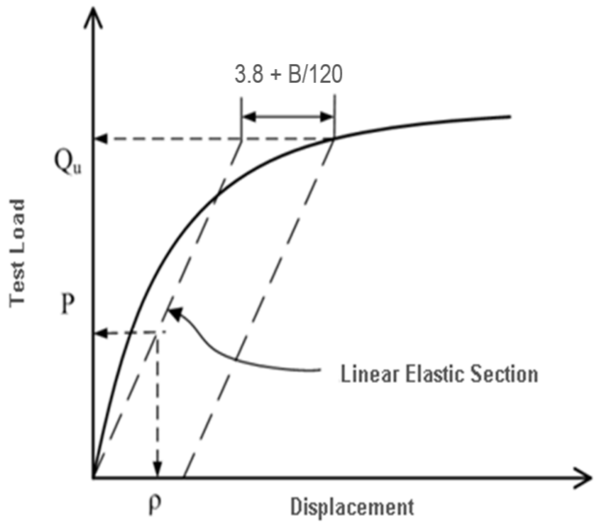

Fig. 5 Schematic for Davisson interpretation method

or

$$\alpha = f_s / \sqrt{q_u} \tag{2}$$

4. Correlation of α versus q_u

Using Eq. (1) and the pile load test data gathered for the value of α, the computation result obtained using the Davisson method, which includes the average results of the gathered data from 41 single pile reports, is shown in Fig. 6. The data were plotted into a (a) general coordinate axes, (b) semi-logarithmic axes, and (c) full-logarithmic axes to determine the best trend for each of the axes. Table 5 shows the statistical analysis to compare the three equations developed for each coordinate axis. In these figures and tables, the statistical results of coefficient of determination (r^2), standard deviation (SD), and coefficient of variation (COV) are also listed.

The results of the statistical analysis presented the three coordinate axes with varying reliability. A low COV of an equation indicates a high reliability of the equation to be utilized. Table 5 presents the statistical results of the regression analysis performed in the study, which shows that the three coordinate equations computed yielded comparable reliability. These coefficients of variabilities are between 0.88 and 0.95 and will be used to measure the acceptability of the derived model and compare the model derived for the α–$\sqrt{q_u}$ relationship in the following sections.

Table 5 Statistical results of the α–q_u relationships

Coordinate form	Regression equation	n	r^2	SD	COV
General coordinate	$\alpha = 0.06 + 0.11/q_u$	41	0.86	0.19	0.94
Semi-logarithmic coordinate	$\alpha = 0.28 - 0.31 \cdot \log q_u$		0.73	0.18	0.88
Full logarithmic coordinate	$\log \alpha = - 0.70 - 0.70 \cdot \log q_u$		0.90	0.19	0.95

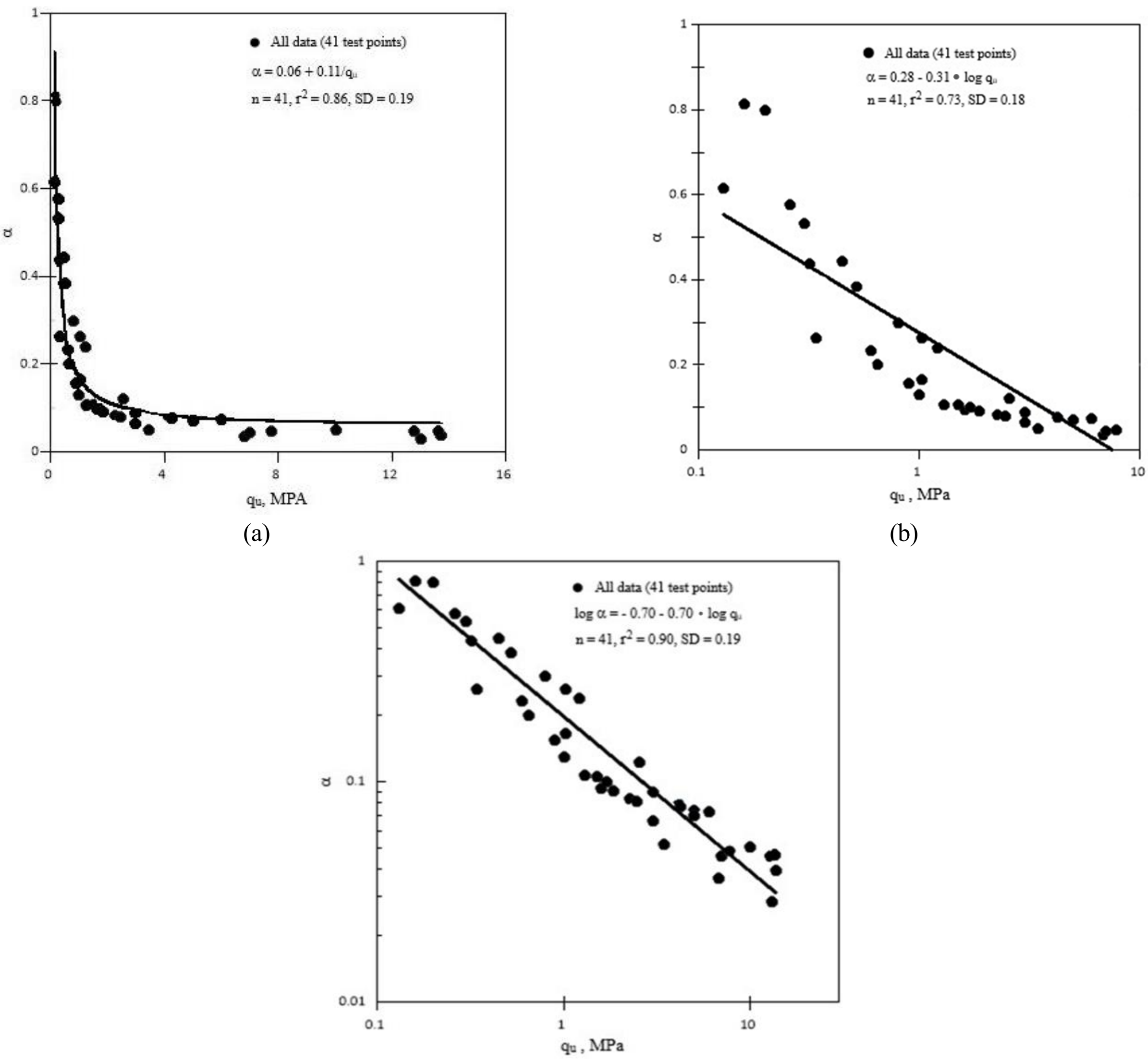

Fig. 6 α–q_u relationships for three analysis modes

5. Correlation of α versus $\sqrt{q_u}$

The analysis presented in this section is commonly used in determining the unit side resistance of pile foundation socketed into rock sections, as shown in Eq. (2). The difference is that the uniaxial compressive strength is analyzed by its root. The new data were then plotted into (a) general coordinate, (b) semi-logarithmic, and (c) full-logarithmic axes to determine the best trend, as shown in Fig. 7.

Table 6 indicates the statistical analysis to compare the regression equations derived from the three coordinate axes used in the study. As explained in the previous section, an equation with low *COV* results in the high reliability of the equation to be utilized. As shown in Table 6, the three coordinate equations also yielded comparable reliability. These coefficients of variabilities are between 0.25 and 0.27 and will be compared with the statistical values computed for the α–q_u relationship to determine the reliable relationship between the two.

Table 6 Statistical results of the α–$\sqrt{q_u}$ relationships

Coordinate form	Regression equation	n	r^2	SD	COV
General coordinate	$\alpha = 0.11 + 0.08/\sqrt{q_u}$	41	0.52	0.05	0.26
Semi-logarithmic coordinate	$\alpha = 0.20 - 0.16 \cdot \log[\sqrt{q_u}]$		0.45	0.04	0.25
Full logarithmic coordinate	$\log \alpha = -0.71 - 0.41 \cdot \log[\sqrt{q_u}]$		0.50	0.05	0.27

6. Comparison of α versus q_u and $\sqrt{q_u}$

Based on the analysis results, the regression equation developed on each of the coordinate axes computed can be used to evaluate side resistances of drilled shafts socketed into rocks because they produced reliability based on the design needs. The coefficient of variance (*COV*) is used to measure the consistency of the equation for the determination of the improved relationship. The comparison of statistical data in Tables 5 and 6 shows that the results of regression equations developed in the α–$\sqrt{q_u}$ relationship

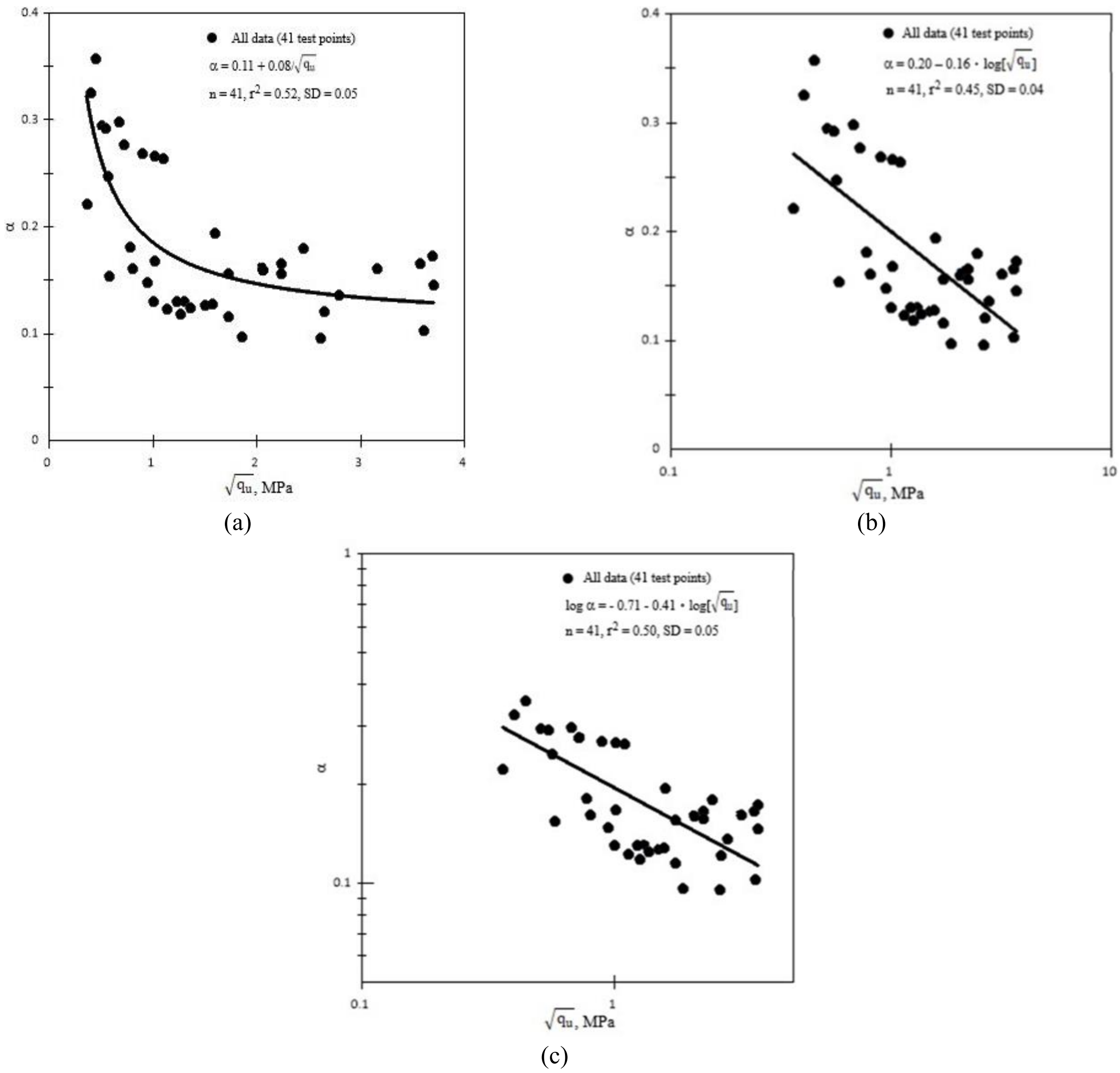

Fig. 7 α–$\sqrt{q_u}$ relationships for three analysis modes

have much lower COV than that of the α–q_u relationship. Therefore, the α– $\sqrt{q_u}$ relationship yielded better correlation than that of the α–q_u relationship for the general, semi-logarithmic, and full logarithmic coordinate axes.

7. α-$\sqrt{q_u}$ - *RQD* Relationships

As previously described, lithology, rock mass conditions, and pile surface conditions may be the factors that influence the friction resistance. Among these factors, *RQD* is the most commonly used factor in geotechnical community. *RQD* is a measure of the quality of rock core taken from a borehole and signifies the degree of fracture or jointing in rock mass measured in percentage. In addition, *RQD* is easily acquired from boring profile data. Therefore, the *RQD* values are incorporated to the α–$\sqrt{q_u}$ relationship to explore its influence. The study also utilized the general coordinate system for the α-$\sqrt{q_u}$–*RQD* relationship because

Table 7 Rock classification using *RQD* (Peck *et al.* 1974)

RQD (%)	Rock Mass Classification
0 ~ 25	Very poor
25 ~ 50	Poor
50 ~ 75	Fair
75 ~ 90	Good
90 ~ 100	Excellent

the three-coordinate systems demonstrated comparable reliability for the α-$\sqrt{q_u}$ relationship, but the general axis is the most commonly used in engineering design practice. Thus, the study utilized the general coordinate data among the three coordinate systems.

The sorted *RQD* classification is based on Peck *et al.* (1974), and the rock sections are classified into five categories, as shown in Table 7. Fig. 8 shows the α -$\sqrt{q_u}$ relationships for various *RQD* classifications. Fig. 8(a) shows that 75%-90% and 90-100% RQD graphs have the

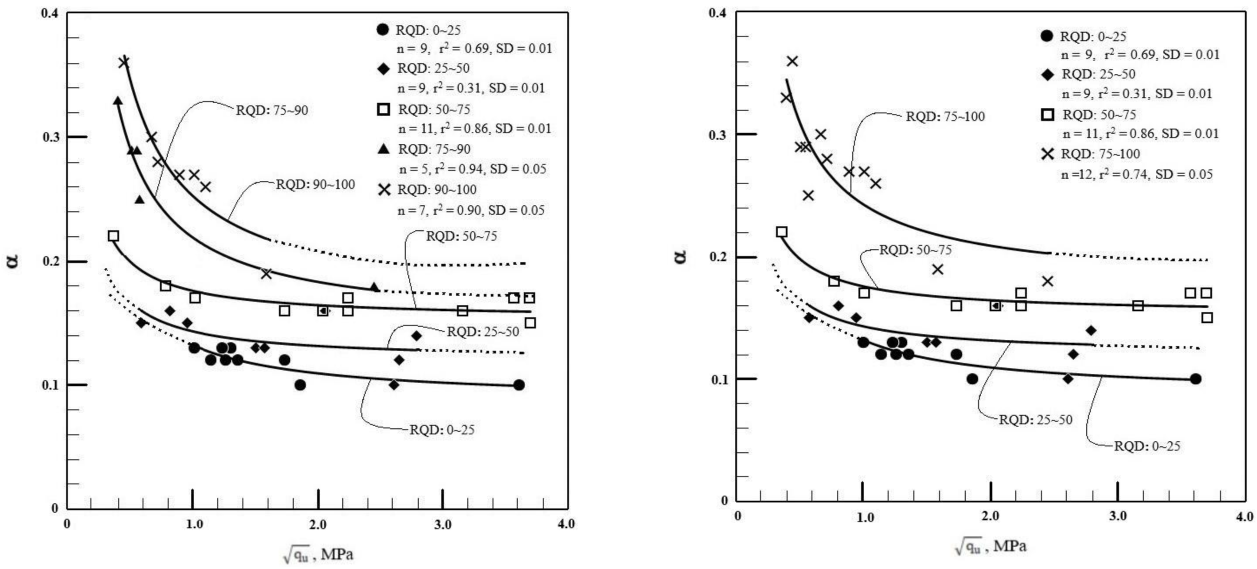

(a) (b)

Fig. 8 α–$\sqrt{q_u}$-*RQD* correlations

Table 8 Statistical results of α-$\sqrt{q_u}$ -*RQD* correlations

RQD (%)	Regression equation	n	r^2	*SD*	*COV*
0~25	$\alpha = 0.09 + 0.05/\sqrt{q_u}$	9	0.69	0.01	0.09
25~50	$\alpha = 0.12 + 0.02/\sqrt{q_u}$	9	0.31	0.01	0.07
50~75	$\alpha = 0.15 + 0.02/\sqrt{q_u}$	11	0.86	0.01	0.09
75~90	$\alpha = 0.15 + 0.07/\sqrt{q_u}$	5	0.94	0.05	0.20
90~100	$\alpha = 0.16 + 0.09/\sqrt{q_u}$	7	0.90	0.05	0.17
(75~100)[1]	$\alpha = 0.18 + 0.07/\sqrt{q_u}$	12	0.74	0.05	0.16

[1]New equation where *RQD* 75-90% and 90-100% are joined into one equation

same trend and can be consolidated into one classification, that is, 75%-100% RQD value, as shown in Fig. 8(b). From Fig. 8, it can be found that the trend is obvious that a large *RQD* leads to a high α value. It is consistent with the general supposition. The α–$\sqrt{q_u}$-*RQD* correlations can be used to select the value of α precisely if *RQD* is given. This correlation can also be regarded as an alternative analysis for traditional α–$\sqrt{q_u}$ correlations. Table 8 lists the regression equations and statistical results of α–$\sqrt{q_u}$ correlation for various *RQD* classifications.

8. Conclusions

This study utilized a large number of load test data to explore side resistances of drilled shafts socketed into rocks. Representative analytical models were comprehensively examined using measured results. Rock quality classification was further considered in the analysis model. The following design recommendations for engineering practice are proposed based on the evaluation.

The study developed a relationship between α–q_u and α–$\sqrt{q_u}$. These relationships were further investigated by plotting the computed values on three coordinate systems, including general, semi-logarithmic, and full logarithmic. The comparison of the statistical data of each relationship proved that the α–$\sqrt{q_u}$ relationship in all its coordinate forms is more accurate for the analysis of drilled shafts socketed into rocks due to its lower *COV* than that of α–q_u.

The α–$\sqrt{q_u}$ correlation is suggested for the design. With the discretion of the design requirements, the recommended correlation has the regression equation of $\alpha = 0.11 + 0.08/\sqrt{q_u}$ with n = 41, r^2 = 0.52, *SD* = 0.05, and *COV* = 0.26 for the general coordinate system; $\alpha = 0.20 - 0.16 \cdot \log[\sqrt{q_u}]$ with n = 41, r^2 = 0.45, *SD* = 0.04, and *COV* = 0.25 for the semi-logarithmic form; and $\log \alpha = -0.71 - 0.41 \cdot \log[\sqrt{q_u}]$ with n = 41, r^2 = 0.50, *SD* = 0.05, and *COV* = 0.27 for the full-logarithmic coordinate system.

The current study utilized the general coordinate equation of α–$\sqrt{q_u}$ and divided the data based on the *RQD* of each rock type gathered to form better prediction equations for the design and further specify the analysis performed. The newly developed α–$\sqrt{q_u}$-*RQD* correlations can be regarded as an alternative analysis method for the drilled shaft design. These correlations can be used to select the required α value precisely if *RQD* is given.

Acknowledgments

This study was supported by the Ministry of Science and Technology, Taiwan, under contract number: MOST 107-2221-E-033-014.

References

American Association of State Highway and Transportation Official (1992), *Standard Specifications for Highway Bridges*, Washington, U.S.A.

Asem, P. and Gardoni, P. (2019a), "A load transfer function for the side resistance of drilled shafts in soft rock", *Soils Found*., **59**(5), 1241-1259. https://doi.org/10.1016/j.sandf.2019.04.006.

Asem, P. and Gardoni, P. (2019b), "Evaluation of peak side resistance for rock socketed shafts in weak sedimentary rock from an extensive database of published field load tests: A limit state approach", *Can. Geotech. J.*, **56**(12), 1816-1831. https//doi.org/10.1139/cgj-2018-0590.

Chen, X.Y., Zhang, M.Y. and Bai, X.Y. (2019), "Axial resistance of bored piles socketed into soft rock", *KSCE J. Civ. Eng*., **23**(1), 46-55. https//doi.org/10.1007/s12205-018-0942-5.

Chen, Y.J. and Fang, Y.C. (2009), "Critical evaluation of compression interpretation criteria for drilled shafts", *J. Geotech. Geoenviron. Eng*., **135**(8), 1056-1069. https://doi.org/10.1061/(ASCE)GT.1943-5606.0000027.

Chen, Y.J. and Kulhawy, F.H. (1994), "Case history evaluation of drilled shafts behavior", Report TR-104601, Electric Power Research Institute, Palo Alto, U.S.A.

Chen, Y.J. and Kulhawy, F.H. (2003), "Evaluation of undrained side and tip resistances for drilled shafts", *Soil Rock Amer*., **2**, 1963-1968.

Chen, Y.J., Liao, M.R., Lin, S.S., Huang, J.K. and Marcos, M.C. (2014), "Development of an integrated web-based system with a pile load test database and pre-analyzed data", *Geomech. Eng*., **7**(1), 37-53. http://doi.org/10.12989/gae.2014.7.1.037.

Chen, Y.J., Lin, S.S., Chang, H.W. and Marcos, M.C. (2011), "Evaluation of side resistance capacity for drilled shafts", *J. Mar. Sci. Technol*., **19**(2), 210-221.

Davisson, M.T. (1972), "High capacity piles", *Proceedings of the Lecture Series on Innovation in Foundation Construction,* Chicago, Illinois, U.S.A., January-May.

Hooley, P. and Lefroy-Brooks, S.R. (1993), "The ultimate shaft frictional resistance mobilized by bored piles in over consolidated clays and socked into weak and weathered rock", *Eng. Geol. Sp. Publ*, (8), 447-455.

Horvath, R.G., Kenney, T.C. and Kozicki, P. (1983), "Methods of improving the performance of drilled piers in weak rock", *Can. Geotech. J*., **20**(4), 758-772. https://doi.org/10.1139/t83.

Hsiao, C.C. (2018), "Evaluation of side resistance for drilled shafts socketed into rock", Master Thesis, Chung Yuan Christian University, Taoyuan, Taiwan.

Kaderabek, T.J. and Reynolds, R.T. (1981), "Miami limestone foundation design and construction", *J. Geotech. Eng. Div*., **107**(7), 859-872. https://doi.org/10.1016/0148-9062(81)90663-X.

Ku, C.S., Weng, J.Y., Liu, X.Z. and Lin, X.H. (2004), "Study on side resistance of soft rock foundations", *Proceedings of the Rock Engineering Symposium*, Tamsui, Taiwan.

Kulhawy, F.H. and Goodman R.E., (2005), *Foundation in Rock*, in Ground Engineers Reference Book, Butterworth and Co. Ltd.

Marcos, M.C. and Chen, Y.J. (2019), "Evaluation of side resistance of driven precast concrete piles", *Mater. Sci. Eng*., **658**(1), 012005. https://doi.org/10.1088/1757-899X/658/1/012005.

Peck, R.B., Hanson, W.E. and Thornburn, T.H. (1974), *Foundation Engineering*, 2nd Ed., John Wiley and Sons, Inc., New York, U.S.A., 361-371.

Qian, Z.Z., Lu, X. L., Yang, W.Z. and Cui, Q. (2016), "Comparative field tests on uplift behavior of straight-sided and belled shafts in loess under an arid environment", *Geomech. Eng*., **11**(1), 141-160. https://doi.org/10.12989/gae.2016.11.1.141.

Rodgers, M., McVay, M., Horhota, D., Sinnreich, J. and Hernando, J. (2018), "Assessment of shear strength from measuring while drilling shafts in Florida limestone", *Can. Geotech. J*., **55**(8), 1154-1167. https://doi.org/10.1139/cgj-2017-0321.

Rowe, R.K. and. Armitage, H.H. (1987), "A design method for drilled piers in soft rock", *Can. Geotech. J*., **24**(1), 126-142. https://doi.org/10.1139/t87.

Stas, C.V. and Kulhawy, F.H. (1984), "Some observations on undrained side resistance of drilled shafts", *Proceedings of the 1989 Foundation Engineering Conference*, Evanston, Illinois, U.S.A., June.

Yang, Z.Y., Shiau, J.Q., Ching, J.Y., Lee, Y.S. and Chen, C.J., (2010), "Side resistance of pile socketed into rock in Taiwan area", *Proceedings of the Rock Engineering Symposium,* Kaohsiung, Taiwan.

Zhang, B., Mei, C., Huang, B., Fu, X., Luo, G. and Lv, B. (2017), "Model tests on bearing capacity and accumulated settlement of a single pile in simulated soft rock under axial cyclic loading", *Geomech. Eng*., **12**(4), 611-626. https://doi.org/10.12989/gae.2017.12.4.611.

CC